Gas Production from Unconfined Class 2 Hydrate Accumulations in the Oceanic Subsurface

George J. Moridis and Michael Kowalsky

Lawrence Berkeley National Laboratory, Earth Sciences Division, 1 Cyclotron Rd., Berkeley, CA 94720, U.S.A.
GJMoridis@lbl.gov

Keywords: gas hydrate, production, depressurization, thermal stimulation

Abstract

Unconfined Class 2 hydrate accumulations in the oceanic subsurface are characterized by mobile saline water zones enveloping the hydrate-bearing formation and by the absence of impermeable layers to vertical flow. In this paper, we evaluate the gas production potential of such deposits using both single-well and five-spot well configurations. Single-well production is based on depressurization-induced dissociation of the hydrates, whereas the five-spot configuration involves both depressurization at the production wells and thermal stimulation at the injection wells. The results of the study indicate that unconfined Class 2 hydrate accumulations are among the most challenging targets for gas production because (a) the absence of confining boundaries limits the effectiveness of depressurization, (b) gas production is accompanied by the production of very large volumes of water, and (c) thermal stimulation, when employed, requires substantial energy inputs. The amount of produced gas is limited in both the single-well and the five-spot configurations, and is significantly smaller than the total volume of gas released in the formation. For the five-spot configuration, hydrate dissociation releases relatively large amounts of gas into the reservoir, but these are not readily recoverable. Gas production is also significantly affected by the initial hydrate saturation in the hydrate-bearing sediment.

Introduction

Background

Gas hydrates are solid crystalline compounds in which gas molecules are lodged within the lattices of ice crystals. Vast amounts of hydrocarbons are trapped in hydrate deposits [Sloan, 1998]. Such deposits occur in two distinctly different geologic settings where the necessary low temperatures and high pressures exist for their formation and stability: in the permafrost and in deep ocean sediments.

Current estimates of the worldwide quantity of hydrocarbon gas hydrates vary widely, and a range between 10^{15} to 10^{18} m^3 has been reported [Sloan, 1998]. These estimates are not the result of a systematic attempt to evaluate hydrate reserves, but are based mainly on data obtained while investigating conventional hydrocarbon resources. Even by the most conservative estimates, the total quantity of gas in hydrates may surpass, by a factor of two, the energy content of the total fuel fossil reserves recoverable by conventional methods [Sloan, 1998]. The magnitude of this resource commands attention because it could make hydrate reservoirs a substantial future energy resource. The potential importance of hydrates is further augmented by the environmental

attractiveness of natural gas (as opposed to solid and liquid) fuels. Although the current energy economics cannot support gas production from hydrate accumulations by conventional means, their potential clearly demands further evaluation.

The three main methods of hydrate dissociation for gas production are: (1) depressurization, in which the pressure is lowered to a level lower than the hydration pressure P_H at the prevailing temperature, (2) thermal stimulation, in which the temperature is raised above the hydration temperature T_H at the prevailing pressure, and (3) the use of inhibitors (such as salts and alcohols), which causes a shift in the P_H-T_H equilibrium through competition with the hydrate for guest and host molecules [Sloan, 1998].

The numerical studies of gas production in this paper were conducted using the TOUGH-Fx/HYDRATE model [Moridis et al., 2005a], the successor to the earlier EOSHYDR2 code [Moridis, 2003] for the simulation of the system behavior in hydrate-bearing geologic media. TOUGH-Fx/HYDRATE can model the non-isothermal hydration reaction, phase behavior and flow of fluids and heat under conditions typical of common natural CH_4-hydrate deposits (i.e., in the permafrost and in deep ocean sediments) in complex formations. TOUGH-Fx/HYDRATE includes both an equilibrium and a kinetic model [Kim et al., 1987; Clarke and Bishnoi, 2001] of hydrate formation and dissociation. The model accounts for heat and up to four mass components, i.e., water, CH_4, hydrate, and water-soluble inhibitors such as salts or alcohols. These are partitioned among four possible phases: gas phase, liquid phase, ice phase and hydrate phase. By solving simultaneously the coupled equations of mass and heat balance, hydrate dissociation or formation, phase changes and the corresponding thermal effects are fully described, as are the effects of inhibitors. The model can describe all possible hydrate dissociation mechanisms, i.e., depressurization, thermal stimulation, salting-out effects and inhibitor-induced effects.

Description of the Geologic System

Moridis and Collett [2004] have developed a simple classification system for naturally occurring gas hydrate deposits, describing three classes on the basis of the phase distributions in the immediate vicinity of the hydrate-bearing layer. Class 1 and Class 2 hydrate deposits are characterized, respectively, by a hydrate-bearing layer (hereafter referred to as the HBL) underlain by (a) a two-phase zone involving mobile gas and water, and (b) a single-phase zone of mobile water. Class 3 accumulations are composed of a single zone, the HBL, and are characterized by the absence of an underlying zone of mobile fluids.

In terms of gas production, Class 1 is the most desirable exploitation target because of the favorable relative permeability regime and the thermodynamic proximity to the hydration equilibrium at the highest possible T_H (necessitating only small changes in pressure and temperature to induce dissociation). The desirability of Class 2 and 3 accumulations as gas production targets is less well defined than for Class 1 deposits, and can be a complex function of several factors, including economic considerations, thermodynamic proximity to hydration equilibrium, initial conditions, and environmental concerns [Moridis et al., 2004; Moridis, 2004].

Production from Class 1, Class 2 and Class 3 hydrates from confined permafrost accumulations has been discussed by Moridis and Collett [2004], Moridis et al. [2004], and Moridis [2004]. In this paper, we focus on gas production from a Class 2 hydrate deposit in the oceanic subsurface.

A particular feature of this gas hydrate accumulation is the absence of confining geologic formations. Thus, the HBL is enveloped by permeable sediments that are fully saturated with ocean water. Such a gas hydrate accumulation (hereafter referred to as a Class 2-OU deposit, with the 'O' denoting the oceanic environment and the 'U' the unconfined type of the deposit) can be formed from supersaturation in dissolved CH_4 (emanating from deeper in the oceanic subsurface), and its evolution can be facilitated by the presence of a lower permeability layer, which causes gas to accumulate and to begin forming hydrates. Generally, the bottom of such deposits coincides with the bottom of the hydrate stability zone at the prevailing pressure and temperature.

Class 2-OU hydrate deposits appear to be challenging targets for gas production because the absence of barriers to vertical flow can severely limit the effectiveness of depressurization, the fastest and most efficient method of hydrate dissociation. An additional complication in such deposits is the difficulty in focusing and directing flow through the hydrate (thus allowing an appropriate pressure drop to develop) because the low-permeability HBL can be bypassed if faster flow pathways (through the more permeable bounding layers) are available. If permeability is not a limiting factor (otherwise, cavitation may occur), the production efficiency appears to be adversely affected by the ready availability of practically limitless amounts of water. This condition requires very large (and potentially uneconomical) water production rates to effect a pressure drawdown sufficient to induce hydrate dissociation at an acceptable rate, while the flow of the evolving gas is hampered by an unfavorable relative permeability regime. Note that, in Class 2-OU deposits, the permeability and extent of the water-saturated formation underlying the HBL are generally more important than those of the overlying one because of the low permeability in the HBL. This limits the amount of water that flows to the well from the upper boundary and through the HBL (at least during the initial stages of production), especially when the hydrate saturation and the thickness of the HBL are large.

Although clearly a disadvantage, there is a potential advantage in the availability of large amounts of water during gas production from Class 2-OU hydrate deposits. Because permeability within the hydrate-bearing layer is generally limited, the large proportion of water in the production stream flows toward the producing well mainly from further and deeper in the underlying formation. By appropriate placement of producing wells, this water (which has a high heat capacity and relatively high temperature by virtue of its large flow rate) can provide some of the heat needed to fuel the strongly endothermic hydrate dissociation reaction. An additional potential advantage is that disposal of the produced water in an oceanic environment is expected to pose far less of an environmental challenge than in the sensitive arctic environment. The produced water need not be brought to the ocean surface, but can be safely released above the ocean floor, thus reducing the cost of production.

Objectives

The aim of this study is not to develop a design for efficient gas production from Class 2-OU hydrate deposits. Instead, the main objectives are to provide a first-level estimate of the production potential of such deposits using conventional technologies, to identify the major issues and limitations affecting production, and to obtain a measure of their relative appeal against other hydrate deposit classes.

Case 1: Gas Production from a Single-Well System

Geometry and Conditions of the System

The schematic in Figure 1 describes the geometry of the single-well gas production from a Class 2-OU hydrate accumulation. The thickness of the HBL is a uniform $H = 50$ m over the footprint of the reservoir. The absolute (intrinsic) permeability of the HBL and of the underlying water-saturated stratum is $k = 10^{-12}$ m^2 (1 Darcy), while the absolute permeability of the overlying layer is $k = 10^{-14}$ m^2. The porosity of all three strata is $\phi = 0.38$. The pressure follows a hydrostatic distribution, and is $P = 10.24$ MPa at the bottom of the HBL. The temperature follows the geothermal gradient, and is $T = 11.25$ ^{o}C at the bottom of the HBL. The top boundary (i.e., at $z < 0$, immediately above the HBL) and the bottom boundary (at $z \leq -350$ m) were maintained at constant temperature, pressure, and salinity conditions. The HBL has an areal extent of 1 km^2. In the HBL, the hydrate is pure CH_4-hydrate, and the initial hydrate and water saturations are $S_H = 0.75$ and $S_w = 0.25$, respectively.

Fluids are produced from a single well at a rate of $Q = 36.8$ kg/s (corresponding to an initial rate of 20,000 BPD of water), and are distributed according to their mobilities at the well. The well is completed in the –45 m to –55 m interval. The initial conditions in the HBL and its enveloping layers, as well as the basic pertinent hydraulic and operational parameters, are listed in Figure 1.

The water released during dissociation continuously dilutes the salinity of the native reservoir water. Because this is a localized phenomenon concentrated where flow (and, under the conditions of the proposed scheme, maximum dissociation) occurs, salinity could not be ignored in this analysis. Note that the salinity level in the native pore water of an oceanic hydrate accumulation can be significant, causing a 1.4 ^{o}C decrease in the dissociation temperature [Dallimore et al.,1999] at the prevailing pressure of 10.24 MPa.

Domain Discretization and Simulation Specifics

To describe this single-well problem, a cylindrical system was used, extending to an outer impermeable boundary at $R_b = 564.19$ m, which corresponds to an area of 1 km^2. The domain was discretized in 38 x 36 subdomains in (r, z), resulting in a total of 1214 gridblocks. Because the hydrate dissociation reaction was assumed to occur at equilibrium, the four equations per cell (mass balance equations of H_2O, CH_4 and salt, plus the heat balance equation) resulted in a system of 4856 equations.

The well is represented as a domain of porosity $\phi = 1$, very high vertical permeability ($k_z = 10^{-8}$ m^2), and of horizontal permeability equal to that of the formation in the completed section of the well and zero elsewhere. The distribution of fluid production along the completed section of the well is determined by the phase permeability regimes in the vicinity of the wellbore when fluids are withdrawn at a mass flow rate Q applied at the well cell immediately above the completed section of the well. The production period is 4 years.

The phase relative permeabilities follow a modification [Moridis et al., 2005a] of the model of Stone [1970], with an irreducible water saturation of $S_{wr} = 0.2$, irreducible gas saturation $S_{gr} = 0.02$, and an exponent $n = 3.572$. The capillary pressure was computed using the method of Parker et al. (1987) with $S_{wr} = 0.2$, $\alpha = 3$ m^{-1}, and $n = 1.65$. These values were based on data

obtained during the Mallik field test of gas production from a permafrost hydrate deposit [Moridis et al., 2005b].

Results of the Single Well Study

The fluid production from the single well leads to depressurization-induced hydrate dissociation. Figure 2 shows the evolution over time of the rate of CH_4 release into the reservoir and the rate of CH_4 production at the well, expressed as ST m^3/day. The gas production rate at the well exhibits oscillations, but the average remains roughly constant during the entire production period. The gas release rate into the reservoir is marked by an initial steep increase, followed by a decline and eventual stabilization. The oscillations in both curves are caused by discretization effects and heat transfer limitations affecting the dissociation reaction. Dissociation is followed by a pressure increase (caused by the gas release) and a drop in temperature (due to the strongly endothermic nature of the dissociation reaction), and results in the steep drop in the release rate and the production rate because of a shift in the dissociation P_H-T_H relationship (see Figure 3). As more heat becomes available (through conduction and fluid advection), the dissociation rate begins increasing. The oscillations are exacerbated by the finite size of the elements into which the simulation domain is subdivided.

Figure 4 shows the cumulative volumes (expressed as ST m^3) of hydrate-originating CH_4 released during the depressurization-induced dissociation and the cumulative gas volume produced from the well over the four-year duration of the study. A comparison of these curves to the ones of the corresponding rates in Figure 2 indicates that the rate fluctuations are attenuated in the cumulative volume curves, which appear remarkably smooth.

Review of Figures 2 and 4 indicates that the amount of produced gas represents a small fraction (about $1/8^{th}$) of the amount of gas released from dissociation. In essence, this means that gas continuously accumulates into the reservoir during the four-year production period. Despite the gas accumulation, the gas reaching the well does not increase over time (because of an adverse gas relative permeability regime) but remains constant (as demonstrated by the practically linear appearance of the cumulative CH_4 volume curve). This is an undesirable scenario, and indicates that simple depressurization in the lower part of and immediately below the HBL do not appear to be a very promising production method. This observation is clearly supported by the magnitude of the CH_4 production rate (about 100 ST m^3/day), which is very low compared to the roughly 3,150 m^3/day of water produced in the process. The lack of appeal of gas production from the single-well depressurization of a Class 2-OU deposit would persist even if the production rate equaled the entire CH_4 release rate in the reservoir.

Effect of the Initial S_H in the HBL

Figure 5 shows the evolution of the cumulative volumes (expressed as ST m^3) of produced CH_4 and of the CH_4 released in the reservoir over the four-year production period when the initial S_H = 0.375, i.e., half of that in the base simulations of Figures 2 and 4. Comparison of Figures 4 and 5 indicate that production from a Class 2-OU deposit with a lower initial S_H is even less appealing. The cumulative gas production decreases with S_H. In this case, the lower initial S_H leads to higher S_w, and, consequently higher water permeability, which allows more flow through the HBL (most of which is bypassed in the higher S_H case), and more effective depressurization of the hydrate. The increase in gas production (as a larger HBL volume becomes available for gas release) is countered by the smaller amount of hydrate (i.e., the CH_4 source) and the increasingly limited flow through the HBL as the hydrate near the well dissociates. As in the

case of higher initial S_H, the produced CH_4 volume represents a rather small fraction of the released volume, and increases roughly linearly with time.

Note that, because of differences in the formation process (and the fact that the presence of hydrates in oceanic porous media limits mass transfer and further hydrate formation), low hydrate saturations are far more common (and probably the norm) in ocean deposits. This further limits the attractiveness of the Class 2-OU deposits,

Case 2: Gas Production from a Five-Spot Well System

Geometry and Conditions of the System

In Case 2, the geology, geometry, properties and initial saturations distribution of the Class 2-OU hydrate accumulation and its boundary formations remain as in Case 1. The stencil in Figure 6 represents the five-spot well configuration, which involves production and injection wells. The injected fluid was hot water at a temperature of 41 ^oC. Hot water was chosen over steam because the parametric study of McGuire [1981] indicated that the amount of produced gas is less than the estimated fuel consumption when steam is employed. Hot water was injected into the center-well of the five-spot pattern, and reservoir fluids were produced from the four production wells. The obvious advantage of this scheme is that it combines the two most important mechanisms of hydrate dissociation, i.e., depressurization at the production well, and thermal stimulation at the injection well.

In an effort to focus the thermal stimulation and depressurization effects in the vicinity of the hydrate interface, the production well was completed in the 0 to –55 m interval, and the injection well in the 0 to –50 m interval. This configuration offered the advantage of limiting mixing of the injected hot water with the colder native reservoir water, while maximizing the thermal advantages of buoyancy that tends to concentrate the warmer water immediately below (and in contact with) the hydrate interface. Additionally, the completion of the wells in the entire hydrate interval took advantage of the gas buoyancy and the maximized contact with the receding hydrate interface in its vicinity. However, the upper parts of the well intervals did not contribute practically any fluids in the early stages of gas production because of adverse relative permeability conditions.

Domain Discretization and Simulation Specifics

Because of symmetry, only a quarter of the domain was simulated using a 3-D Cartesian system. The side of the simulated quadrant was 100 m. The domain was discretized in 15x15x25 unequally spaced subdivisions in (x,y,z), resulting in a total of 5,625 elements. Assuming equilibrium dissociation, four equations (i.e., components) were considered (CH_4, H_2O, salt, and heat) in each element, leading to a system of 22,500 simultaneous equations. The large size and the complexity of the simulated system made the solution of this problem very computationally demanding.

The well representation, as well as the relative permeability and capillary pressure models and parameters remained as in Case 1. Because only a quadrant of the five-spot pattern in Figure 6 (corresponding to $1/4^{th}$ of the rates in the full system) is simulated, and each five-spot configuration occupies $1/25^{th}$ of the 1 km^2 area of the footprint of the hydrate deposit, the initial mass production rate was Q = 36.8/(4x25) = 0.368 kg/s, but the water injection rate was equal to

the rate of water withdrawal from the production well. Thus, the total production rate from the entire hydrate deposit was equal to that in the single-well system of Case 1. The gas and aqueous phase production rates were determined by the phase relative permeabilities in the production well elements. The simulation was allowed to continue for 4,000 timesteps, at which time the results were to be evaluated and a decision made regarding further continuation of the simulation.

Results of the Five-Spot Study

After 4000 timesteps, the simulation had lasted over three days of continuous execution and had covered a production period of 212 days. Because the results and their pattern were rather well defined, and because the execution time requirements of this problem were very substantial, we decided to terminate the simulation at that point.

Figure 7 shows the evolution over time of the rate of CH_4 release into the reservoir and the rate of CH_4 production at the well, expressed as ST m^3/day. These results correspond to the entire 1 km^2 hydrate accumulation. Comparison to the rates from the single-well production in Case 1 leads to the obvious conclusion that, while the rate of gas release in the reservoir is substantially larger than that in Case 1, the rate of CH_4 production at the well is much lower. Additionally, although the rate of gas release continues increasing (albeit slowly) over the 212-day period of the study, the rate of CH_4 production at the well is either constant or declines slightly.

The lower production rate and the difference in the long-term trend are attributed to two reasons. The first is that the injection and production rates are roughly equal during this period (as evidenced by the very low gas production). This rate parity does not allow significant depressurization at the production well because of the relatively short distance between the injection and production wells, and the speed at which the pressure front advances. Thus, the warm water re-injection prevents a significant pressure drop at the production well, leading to lower hydrate dissociation and a lower CH_4 production rate at the well. Moreover, after a maximum pressure imbalance early in the production period, the pressure tends to a steady-state distribution (though continuously disrupted by the gas release from hydrate dissociation), leading to the constant (or slight decline of) the production rate of CH_4 that originating almost exclusively from depressurization-induced hydrate dissociation near the production well.

The second reason for the low gas production rate (and for the increasing release rate trend) is because gas from the thermally induced dissociation in the vicinity of the injection well has not yet reached the production well because of adverse relative permeability conditions. Thus, most of the gas released in the reservoir is expected to be by thermal dissociation. The slowly and continuously expanding thermal front leads to the slowly increasing (over time) release rate observed in Figure 7. The disparity between CH_4 release (in the reservoir) and production rates, brought about by low depressurization and the limited mobility of the gas from thermal dissociation, are expected to lead to a significant gas accumulation in the reservoir.

The differences in the fluctuations of the rate curves in Figure 7 stem from the origin of gas they represent, and from the different impact of discretization effects. Thus, the release rate curve is expected to affect a relatively large number of elements as the warm water front advances toward the production well, as indicated by the large number of oscillations (denoting finite element size). Conversely, because of the limited impact of depressurization, dissociation is expected to

occur in a limited number of elements, as implied by the few and distinct oscillations in the production rate curve.

The expectations from Figure 7 are confirmed in Figure 8, which shows the evolution over time of the cumulative volume (in ST m^3) of produced CH_4 and of CH_4 released in the entire 1 km^2 deposit. The curves in Figure 8 point to a very substantial gas accumulation in the reservoir, which is not accompanied by a commensurate increase in gas production during the 212 days of simulation. If the reason for this disparity is that the gas from thermal dissociation has not reached the production well during that period, then it is almost inevitable that this will happen at a later time, and will be accompanied by a surge in production. However, the question that has to be asked before further pursuing this venue is whether such an approach holds any appeal, as it tends to indicate over 0.6 of a year of continuous water production, heating and circulation with practically no gas production. Note that, as in Case 1, the cumulative volume curves attenuate the oscillations in the corresponding rate curves, and have a remarkably smooth appearance.

Further consideration of Figures 7 and 8 indicates that the rate of CH_4 release in the reservoir and the corresponding cumulative volume are large and within the range of commercial viability. The obvious issue is whether an appropriate production system can be designed that enables the early access to, and production of, the majority of the released gas. Such a system may involve asymmetric production and injection rates (with injection rate being a fraction of the production rate) or horizontal wells, and are likely to require higher levels of management. Although these studies can hold substantial scientific interest, their appeal is eclipsed by far more promising hydrate targets for gas production, e.g., Class 1 deposits.

Figure 9 shows the pressure distribution in the (a) 3-D five-spot quadrant and (b) along the $x = y$ plane, i.e., the plane passing from the injection and production wells. As expected, the highest pressures are observed in the vicinity of the injection well, and the lowest in the immediate neighborhood of the production well. The temperature distribution in Figure 10 exhibits high temperatures at the injection well, and low temperatures (below the initial $T = 11.25\ ^{o}C$) near the production well, where some depressurization-induced dissociation occurs (see Figure 7).

The gas and hydrate saturations in Figures 11 and 12, respectively, are consistent with each other, with the pressure and temperature distributions of Figures 9 and 10, and with the rates and cumulative volumes of Figures 7 and 8. Minor hydrate dissociation is observed along the bottom of the HBL, consistent with the limited depressurization to which this region is exposed. The highest gas saturation corresponds to the location of maximum hydrate dissociation, and is located near the well of warm water injection. This is consistent with the expectations and deductions from Figures 7 and 8. The main body of the gas saturation front in Figure 11 has not reached the production well after 212 days of production (actually, it has covered less than half the distance between the wells), thus explaining the reason for the low production rate and confirming the source of the majority of the released gas. The maximum pressure is observed at a location above the hydrate interface and of the location of the highest temperature, and is caused by the resistance to flow of the CH_4 (released from thermal dissociation of hydrate) into the low permeability HBL. The increased pressure shifts the equilibrium T_H, and results in hydrate persistence despite the higher temperatures.

Summary and Conclusions

This paper focuses on the study of gas production from Class 2-OU hydrate accumulation, i.e., oceanic deposits characterized by a HBL enveloped by permeable geologic media fully saturated with mobile water. The objectives of this study were to provide a measure of the production potential of such deposits using conventional technologies and to identify the factors limiting production, thus developing the knowledge base for meaningful comparisons of the relative value of such deposits as production targets against those from other hydrate accumulations.

Using a Class 2-OU deposit with an areal footprint of 1 km^2 and a HBL of pure CH_4-hydrate and 50 m thick, two production strategies were investigated. In the first, fluid production from a single well at the center of the reservoir effected depressurization, which led to gas production by inducing hydrate dissociation. The second strategy employed combinations of injection and production wells in a five-spot pattern, and involved both depressurization (at the production wells) and thermal stimulation near the injection wells, through which the produced water (heated to 40 ^oC) was re-injected.

The results of these studies lead to the following conclusions:

(1) In both cases, the CH_4 production rates were practically constant over time, and significantly lower than the rate of gas release into the reservoir. At no time during the simulation period do the release and production curves show any tendency toward convergence or even constant deviation. This indicates that gas accumulates in the reservoir at a rate that increases with time, but the adverse relative permeability regime does not allow ready gas recovery.

(2) As indicated by the trend in the rates, in both cases, the cumulative volumes of produced CH_4 were significantly lower than cumulative volumes of CH_4 released into the reservoir.

(3) Gas production decreases with a decreasing hydrate saturation of the HBL because of reduced availability of hydrate.

(4) The production rate was higher in the case of single-well production because, in the five-spot pattern, the (a) gas produced from the thermal dissociation of hydrate caused by the warm water re-injection is very slow to reach the production well, and (b) the water re-injection does not allow a significant pressure drop, thus reducing the driving force of the depressurization-induced dissociation near the production well.

(5) Conversely, the CH_4 release rate into the reservoir was significantly higher in the five-spot well pattern because of the large volumes of re-injected water as an agent of thermal dissociation. The rather spatially uniform injection of the warm water (a result of the small footprint of the five-spot stencil) increases the effectiveness of thermal dissociation.

(6) Although the volume of CH_4 released from dissociation is large (and within the realm of economic viability) in the case of the five-spot well system, this volume is not readily recoverable using the vertical wells of this conventional configuration. A higher-level of management and/or different well systems (e.g., horizontal wells) may be needed to achieve a more efficient (and economically attractive) recovery from such hydrate deposits.

(7) The production rates in both well configurations are very low, and cannot justify considering Class 2-OU hydrate accumulations as economically viable targets for gas

production. Further study will be needed to develop appropriate production strategies if such deposits are to be targeted for gas recovery.

(8) For all the aforementioned reasons, Class 2-OU hydrate accumulations do not appear to be appealing targets for gas production using conventional technologies, especially when considered against far more promising candidates such as Class 1 deposits.

(9) The main reasons for the limited potential of Class 2-OU hydrate deposits as a gas source are (a) the ineffectiveness of depressurization as the driving force of dissociation in the absence of confining layers, (b) the availability of practically limitless amounts of water in the vicinity of the HBL, necessitating large water production rates for an effective pressure drop, (c) the challenge of focusing and directing water flow through the HBL (easily bypassed if higher permeability pathways through the enveloping boundary layers are available), and (d) the adverse relative permeability to gas flow, as gas attempts to emerge as a mobile free phase in a fast-flowing water-saturated geologic medium.

Acknowledgments

This work was supported by the Assistant Secretary for Fossil Energy, Office of Natural Gas and Petroleum Technology, through the National Energy Technology Laboratory, under the U.S. Department of Energy, Contract No. DE-AC03-76SF00098. The authors are indebted to Timothy Kneafsey and John Apps of LBNL for their insightful review comments.

References

Clarke, M. and P.R. Bishnoi, *Determination of Activation Energy and Intrinsic Rate Constant of Methane Gas Hydrate Decomposition*, **Canadian Journal of Chemical Engineering**, 79(1), 143-147, 2001.

Dallimore, S.R., T. Uchida and T.S. Collett, Eds., Scientific Results from JAPEX/JNOC/GSC Mallik 2L-38 Gas Hydrate Research Well, Mackenzie Delta, Northwest Territories, Canada; Geological Survey of Canada Bulletin 544, 1999.

Kim, H.C., P.R. Bishnoi, R.A. Heideman, and S.S.H. Rizvi, *Kinetics of Methane Hydrate Decomposition,* **Chemical Engineering Science**, 42(7), 1645-1653, 1987.

McGuire, P.L., Methane hydrate gas production: An assessment of conventional production technology as applied to hydrate recovery, Report LA-9102-MS, Los Alamos National Laboratory, Los Alamos, NM, 1981.

Moridis, G.J., M. Kowalsky and K. Pruess, TOUGH-Fx/HYDRATE: A code for the simulation of system behavior in hydrate-bearing geologic media, Lawrence Berkeley National Laboratory, 2005 (LBNL Report No. pending).

Moridis, G.J., T.S. Collett, S.R. Dallimore, T. Inoue, and T. Mroz, *Analysis and Interpretation of the Thermal Test of Gas Hydrate Dissociation in the Mallik 5L-38 Research Well, Mackenzie Delta, Canada*; in **Scientific Results from the Mallik 2002 Gas Hydrate Production Research Well Program, Mackenzie Delta, Northwest Territories, Canada**, (ed.) S.R. Dallimore and T.S. Collett; Geological Survey of Canada, Bulletin 585, 2005.

Moridis, G.J., *Numerical Studies of Gas Production from Class 2 and Class 3 Hydrate Accumulations at the Mallik Site, Mackenzie Delta, Canada*, **SPE Reservoir Evaluation and Engineering,** 7(3), 175-183, 2004.

Moridis, G.J. and T. Collett, *Gas Production from Class 1 Hydrate Accumulations*, in ***Recent Advances in the Study of Gas Hydrates***, C. Taylor and J. Qwan, Editors, Kluwer Academic/Plenum Publishers (Section I, Chapter 6, 75-88), 2004.

Moridis, G.J., T. Collett, S. Dallimore, T. Satoh, S. Hancock and B. Weatherhill, *Numerical Studies Of Gas Production From Several Methane Hydrate Zones At The Mallik Site, Mackenzie Delta, Canada*, **Journal of Petroleum Science and Engineering,** 43, 219-239, 2004.

Moridis, G.J., *Numerical Studies of Gas Production From Methane Hydrates*, **SPE Journal**, 32(8), 359-370, 2003.

Parker, J.C., R.J. Lenhard, and T. Kuppusamy, *A Parametric Model for Constitutive Properties Governing Multiphase Flow in Porous Media***, Water Resources Research**, 23(4), 618-624, 1987.

Sloan, E.D., *Clathrate Hydrates of Natural Gases*, Marcel Dekker, Inc.: New York, NY, 1998.

Stone, H.L., *Probability Model for Estimating Three-Phase Relative Permeability*, **Transactions of the SPE of AIME**, 249, 214-218, 1970.

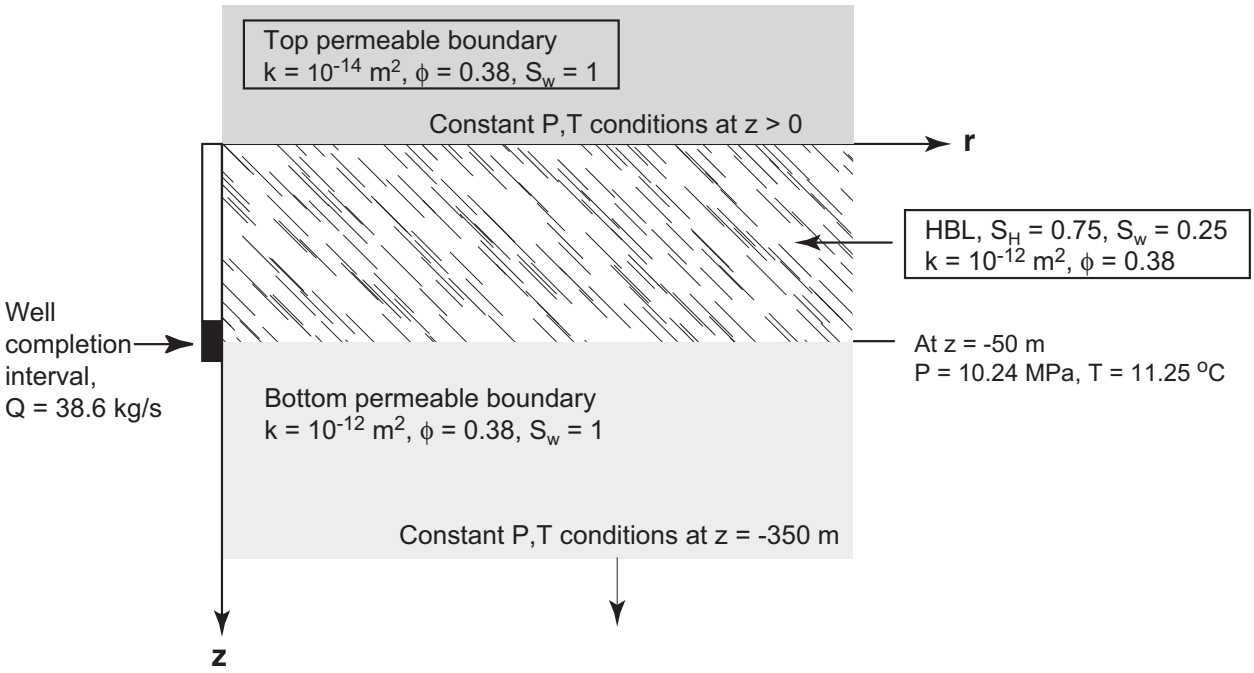

Figure 1. The characteristics and properties of the Class 2-OU formation studied in Case 1.

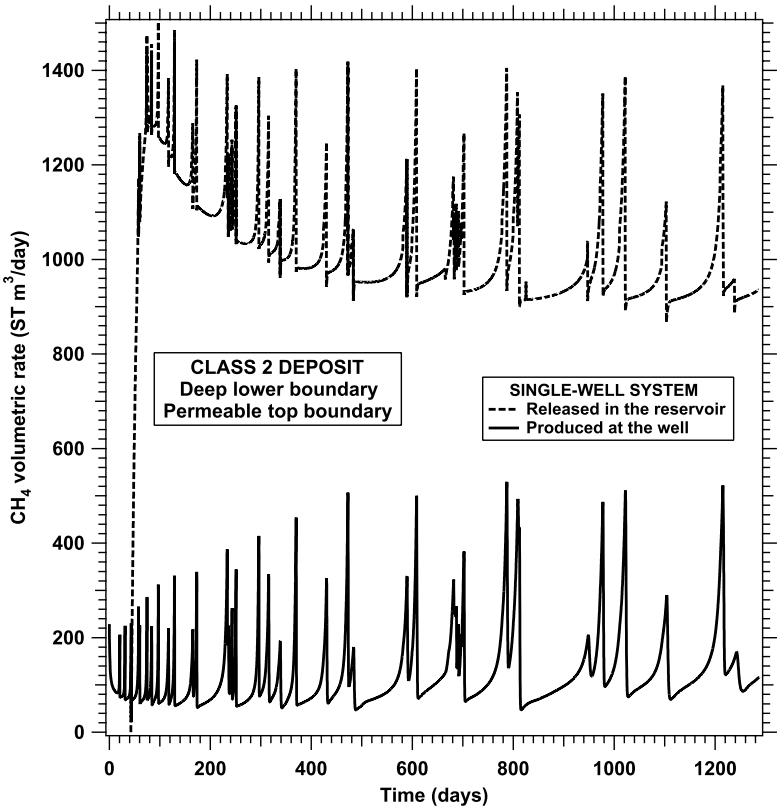

Figure 2. Evolution of the CH_4 production rate and of the rate of CH_4 release (from depressurization-induced hydrate dissociation) into the reservoir during production from a single well in Case 1 ($S_H = 0.75$).

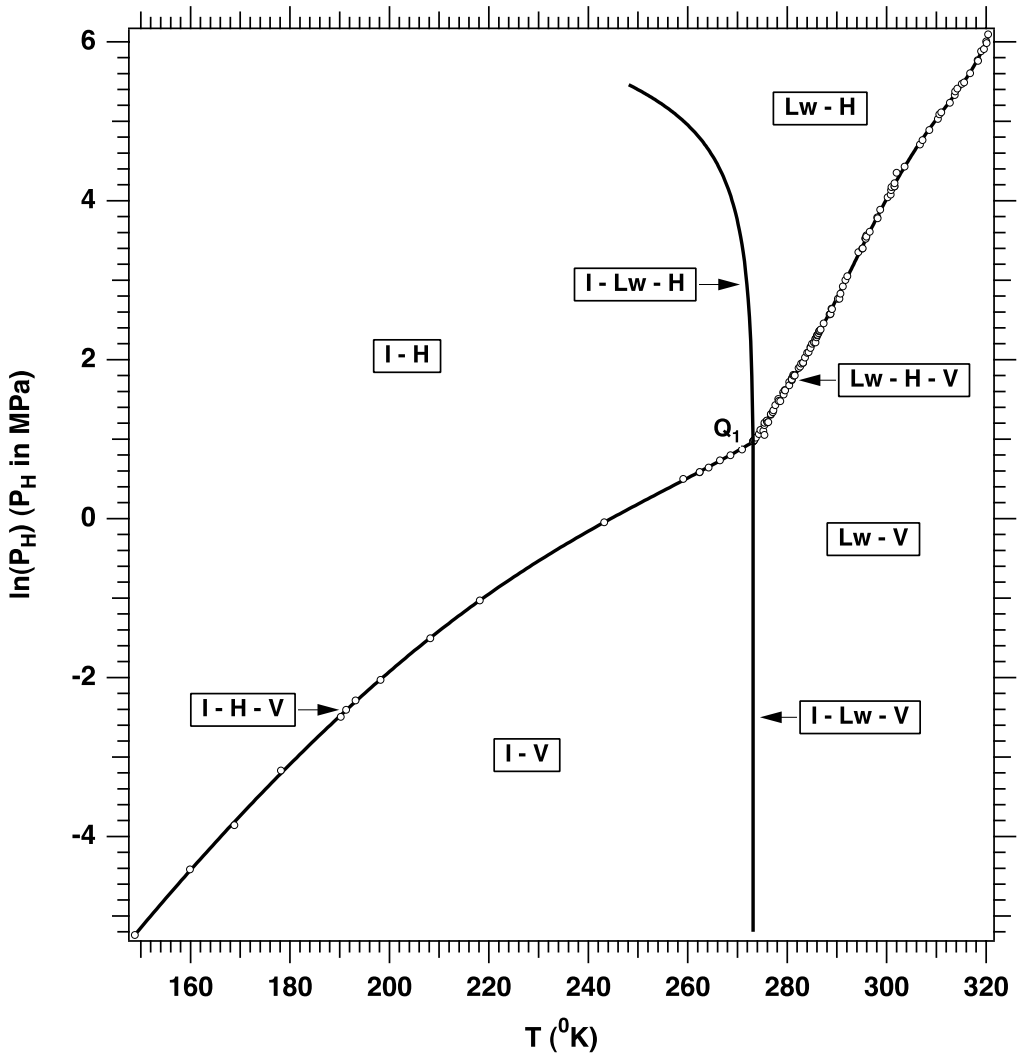

Figure 3. Pressure-temperature equilibrium of the simple methane hydrate [Moridis, 2003].

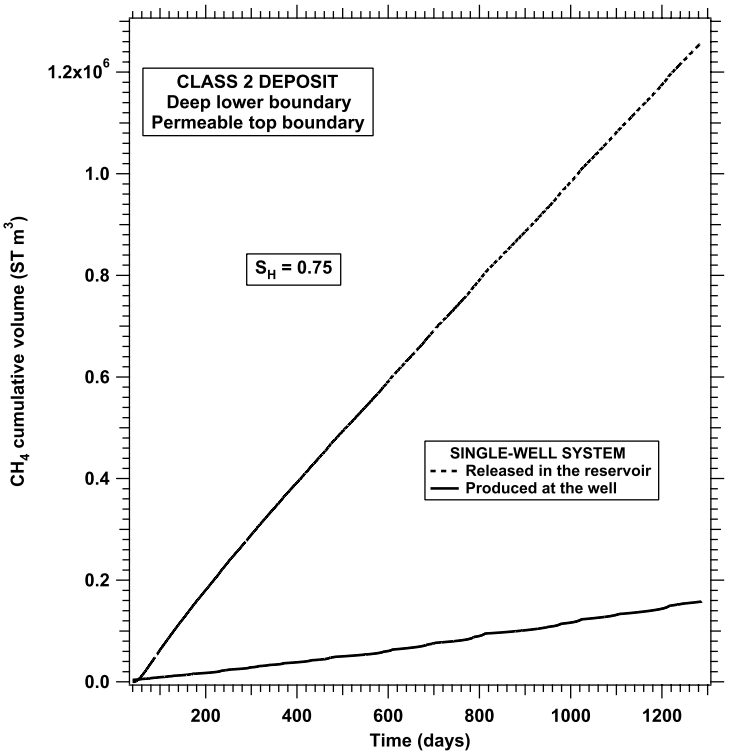

Figure 4. Evolution of the cumulative volumes of produced CH_4 and of CH_4 released into the reservoir during production from a single well in Case 1 ($S_H = 0.75$).

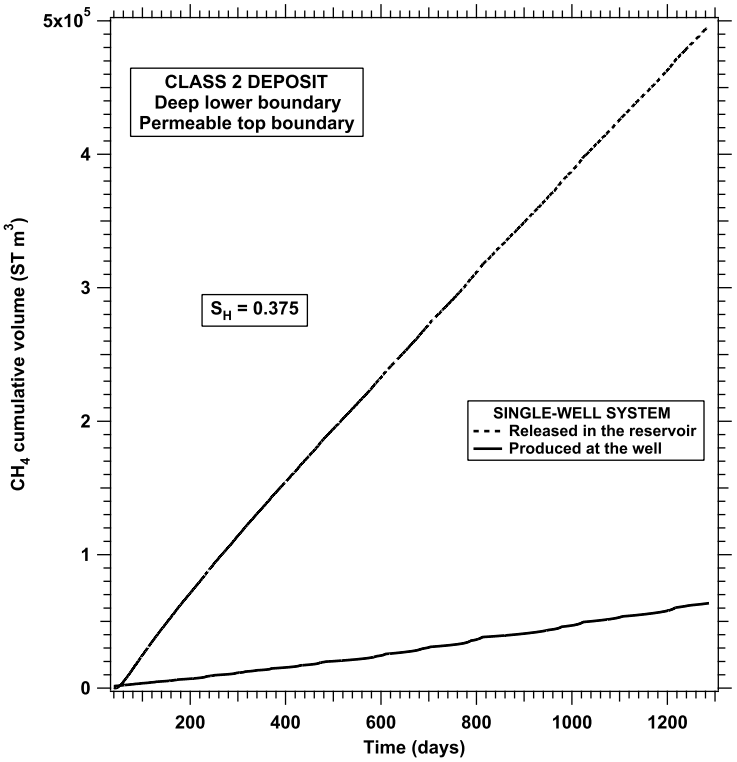

Figure 5. Evolution of the cumulative volumes of produced CH_4 and of CH_4 released into the reservoir during production from a single well in Case 1 ($S_H = 0.375$).

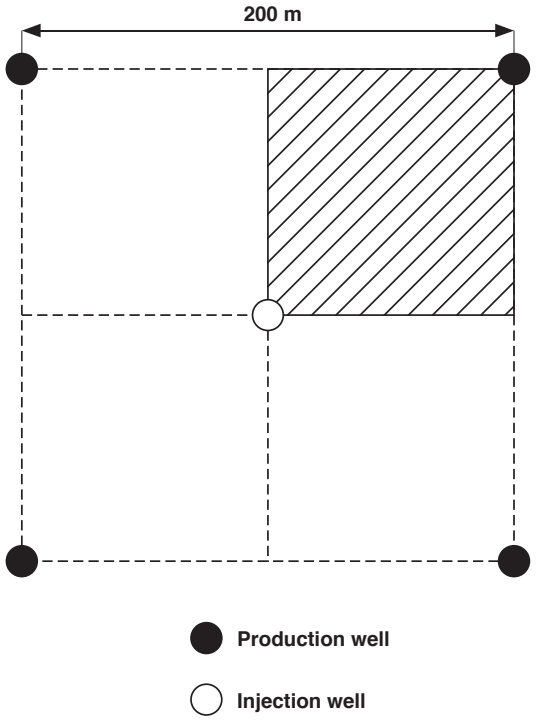

Figure 6 - Five-spot well stencil (pattern) for modeling a 1/4 symmetry subdomain (shaded) in the simulations of Case 2.

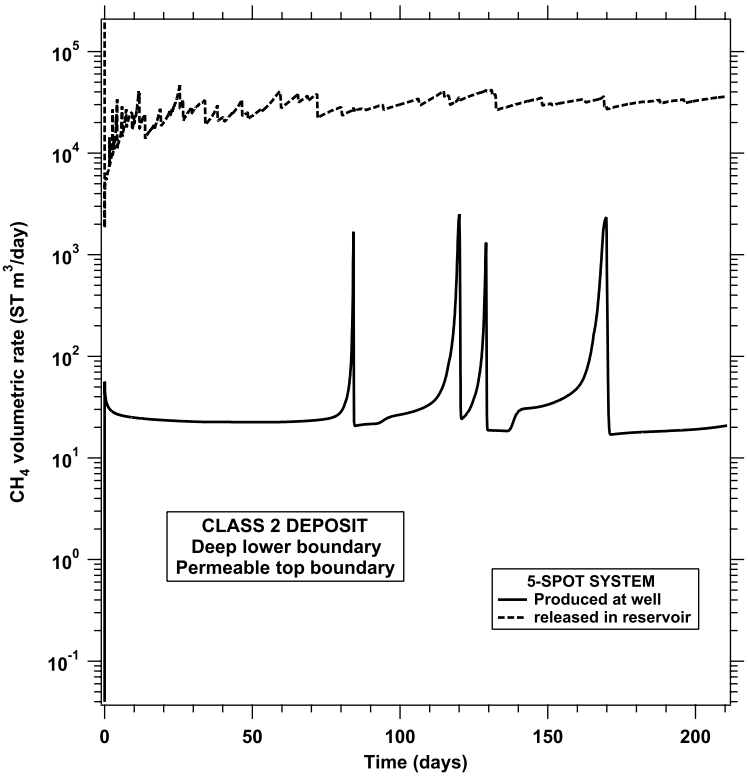

Figure 7. Evolution of the CH_4 production rate and of the rate of CH_4 release into the reservoir during production from a five-spot well system in Case 2 ($S_H = 0.75$).

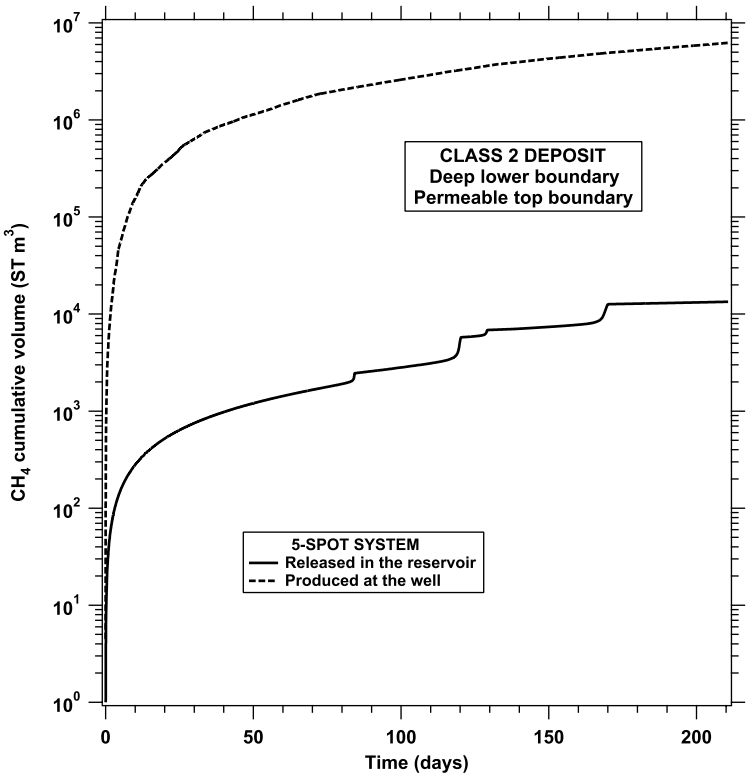

Figure 8. Evolution of the cumulative volumes of produced CH_4 and of CH_4 released into the reservoir during production from a five-spot well system in Case 2 ($S_H = 0.75$).

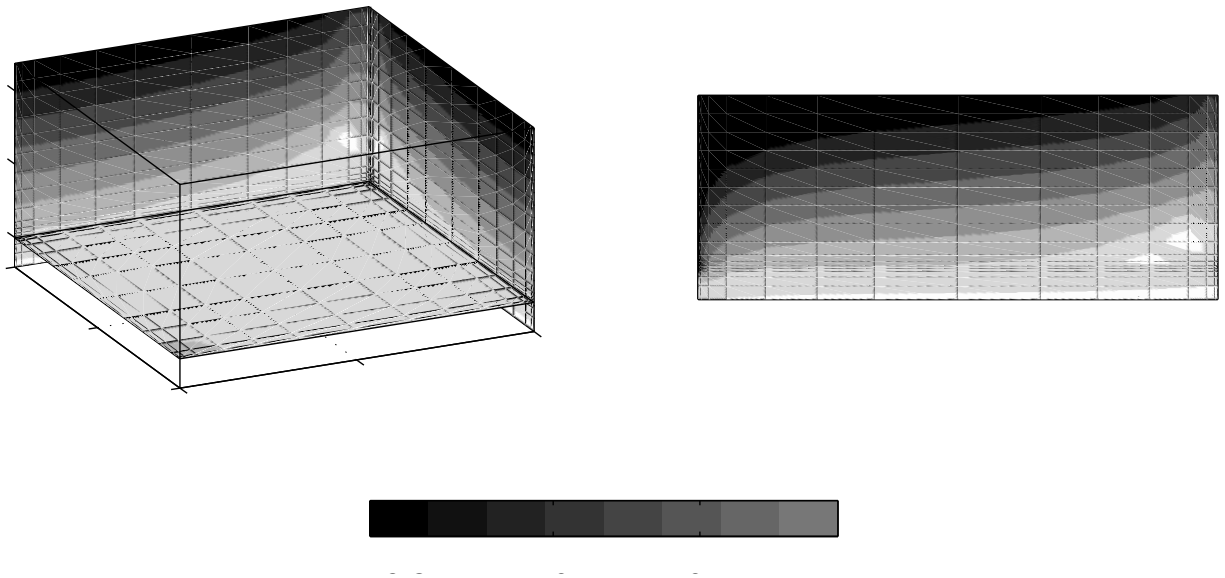

Figure 9. Pressure distributions (a) in the simulated 3-D domain and (b) in the plane defined by the injection and production wells in Case 2.

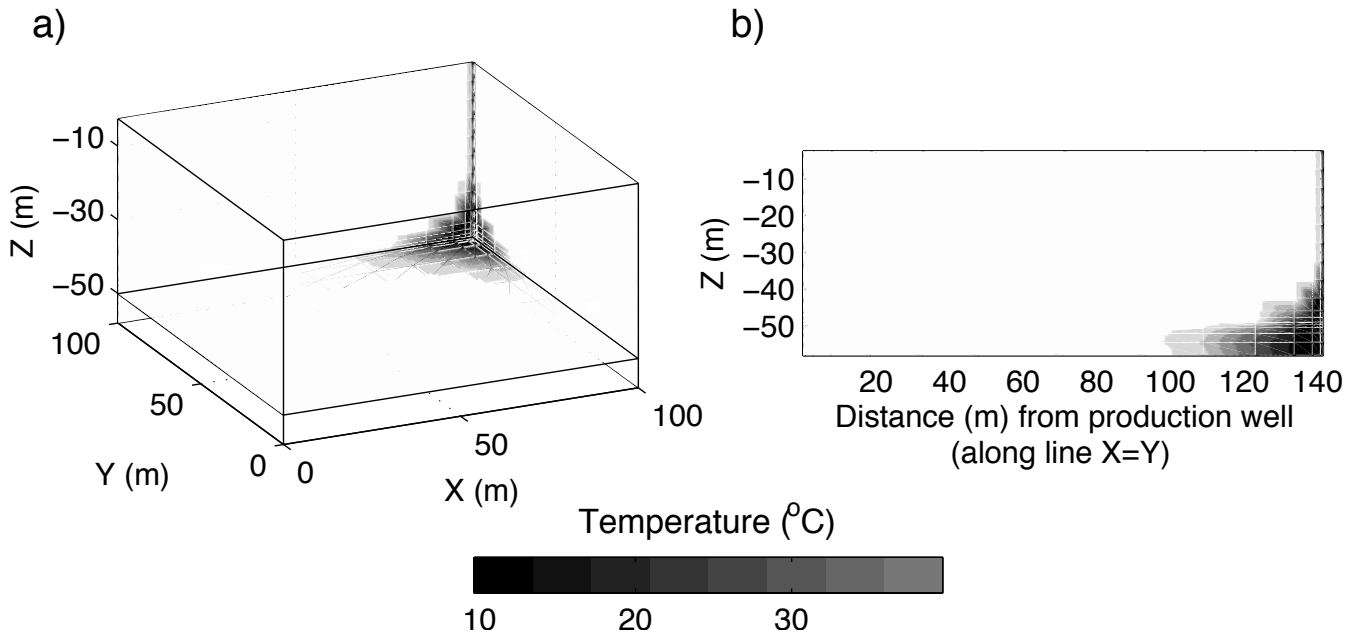

Figure 10. Temperature distributions (a) in the simulated 3-D domain and (b) in the plane defined by the injection and production wells in Case 2.

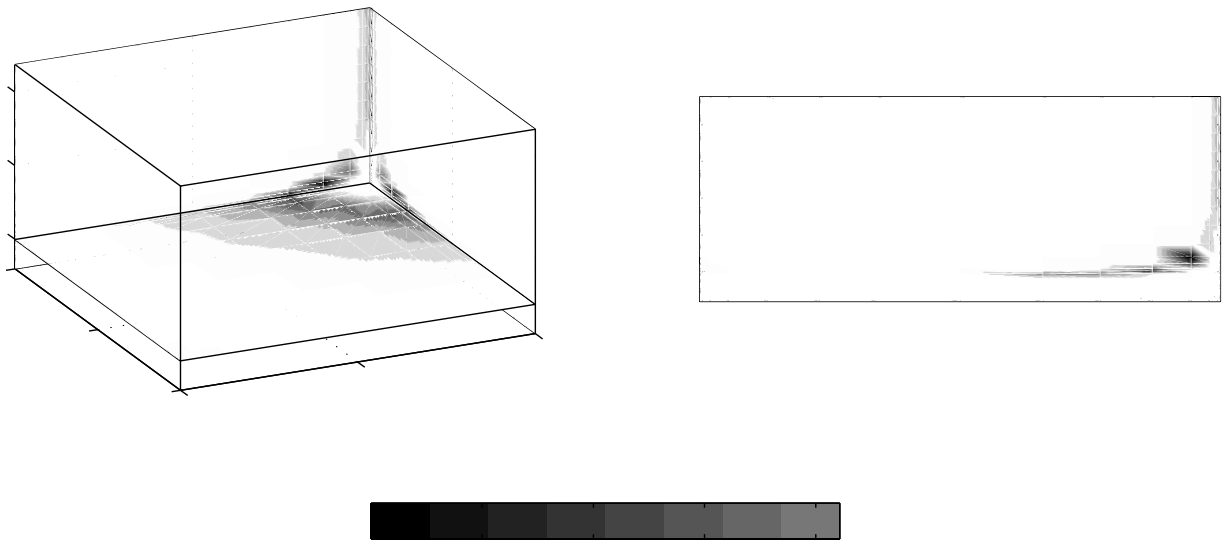

Figure 11. Gas saturation distributions (a) in the simulated 3-D domain and (b) in the plane defined by the injection and production wells in Case 2.

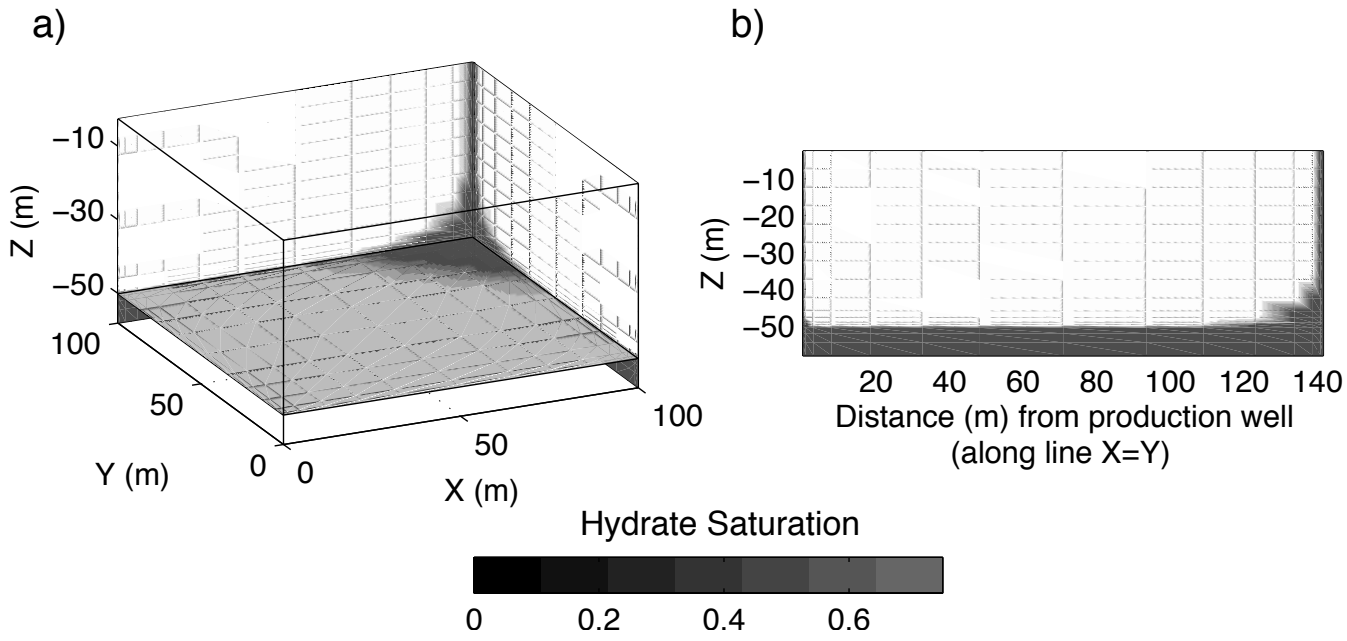

Figure 12. Saturation distributions of the gas hydrate (a) in the simulated 3-D domain and (b) in the plane defined by the injection and production wells in Case 2.